XLVI CILAMCE
VITÓRIA - ES - BRAZIL - 2025
XLVI IBERO-LATIN AMERICAN CONGRESS ON COMPUTATIONAL METHODS IN ENGENEERING

Optimization framework for multi-material mooring lines applied to floating offshore wind turbines

Gabriel R. Hilgert[1], Felipe T. Stumpf[1]

[1]*GMAp, Universidade Federal do Rio Grande do Sul*
Rua Sarmento Leite, 425, 90046-902, Porto Alegre, Brazil
gh_1770@hotmail.com

Abstract. As offshore activities move into deeper and harsher waters, conventional mooring systems face growing limitations. Traditional steel-based designs are heavy, costly, and prone to corrosion, prompting the exploration of alternatives. Lightweight synthetic fibers like polyester (PET), high-modulus polyethylene (HMPE), and polyamide offer advantages in weight and durability but also introduce trade-offs in strength, elasticity, fatigue resistance, and cost. One solution is hybrid mooring lines with combinations of different materials in series. This design balances the strengths of each material while minimizing their weaknesses. However, creating such systems is complex and requires careful tuning of material properties, dimensions, and configurations. This study presents an optimization framework for hybrid mooring systems, using simulations to assess performance under offshore conditions. Tools like OpenFAST are used to evaluate dynamic system responses to waves, currents, and winds. The optimization targets both performance and cost, balancing integrity, stability, and affordability. The approach is applied to floating offshore wind turbines (FOWTs), specifically the OC4 DeepCwind 5 MW platform. The framework identifies optimal configurations for hybrid mooring lines, combining HMPE and polyester segments.

Keywords: floating offshore wind turbines, hybrid mooring lines, optimization, synthetic materials, OpenFAST simulation

1 Introduction

Floating offshore wind turbines (FOWTs) have emerged as a key solution to unlock wind energy potential in deepwater regions where fixed-bottom structures are not feasible, as shown by Jonkman [1], Wang et al. [2]. A critical challenge in FOWT deployment is the design of mooring systems that ensure structural integrity and station-keeping performance while remaining economically viable. Jiang [3], Chevillotte [4], Banfield et al. [5] have shown that Traditional steel-based mooring lines, although widely adopted, are heavy, prone to corrosion, and expensive over the lifecycle of the platform.

To address these challenges, synthetic materials such as polyester, high-modulus polyethylene (HMPE), and polyamide have gained traction due to their favorable weight-to-strength ratios, corrosion resistance, and fatigue performance, as noted by Bastos [6], Bastos et al. [7], da Cruz et al. [8], Stumpf et al. [9]. Nevertheless, each material brings trade-offs in elasticity, cost, creep behavior and dynamic response under operational and extreme conditions (Chevillotte [4], Banfield et al. [5], Sørum et al. [10]). These limitations have encouraged the exploration of hybrid mooring lines, which strategically combine different materials to leverage their respective strengths (Stumpf et al. [9], Ansari [11], Leite et al. [12]).

Designing such hybrid systems is inherently multidisciplinary and complex, requiring robust modeling of hydrodynamic, aerodynamic, structural, and material interactions, as discussed by Hall et al. [13], Hall and Goupee [14]. Quasi-static approaches, though computationally efficient, often fail to capture the dynamic behavior and load exchanges in hybrid configurations, leading to underestimation of fatigue and extreme loads (Hall et al. [13], Abdelmoteleb and Bachynski-Polić [15]). Frequency and time-domain models, when paired with realistic environmental loading and material behavior, including nonlinearity and hysteresis, offer better results (Abdelmoteleb and Bachynski-Polić [15], Al-Solihat and Nahon [16]). Frequency domain analysis, while computationally efficient, requires simplified assumptions about the system's dynamic response, which may not accurately reflect the complex interactions in hybrid mooring lines (Abdelmoteleb and Bachynski-Polić [15]), therefore, time-domain simulations are applied in this study.

To support the design of hybrid mooring systems, this work proposes an optimization framework that integrates simulation tools and material-specific models. The framework uses OpenFAST [17] to simulate the dynamic response of moored FOWTs under combined wind, wave, and current loads, ensuring accurate evaluation of translational and rotational motion, mooring tension, and anchor loads. The optimization process simultaneously minimizes system cost and maximizes structural and dynamic performance metrics.

This methodology is applied to the OC4 DeepCwind 5 MW platform, as described by Robertson et al. [18], a widely adopted benchmark for semi-submersible FOWTs. The hybrid mooring line is composed of HMPE and polyester segments, with the framework identifying optimal length and diameter configurations. The approach offers a scalable solution for future design automation efforts, where population-based algorithms and alternative optimization techniques could enhance the search for optimal mooring solutions across broader design spaces (Leimeister et al. [19], Ja'e et al. [20], Jiang et al. [21]).

2 Optimization framework

The optimization framework proposed in this study seeks to identify an optimal configuration of a hybrid mooring line for a floating offshore wind turbine (FOWT). The framework is designed to use COBYLA (Powell [22]) to simultaneously minimize the total cost of the mooring line and optimize key performance metrics related to the structural integrity and stability of the system.

2.1 Objective functions

The objective function (1) is formulated as a weighted sum of the individual objective functions, normalized by their baseline values. That is,

$$f(\vec{p} \leftarrow \vec{z}) = \sum \frac{w_i f_i(\vec{p})}{F_i^{scale}} = \frac{w_c f_c(\vec{p})}{F_c^{scale}} + \frac{w_d f_d(\vec{p})}{F_d^{scale}} + \frac{w_s f_s(\vec{p})}{F_s^{scale}}, \tag{1}$$

where $f(\vec{p} \leftarrow \vec{z})$ represents the overall objective function, $f_i(\vec{p})$ are the individual objective function values for the input design parameters $\vec{z}$ evaluated as the parsed parameters $\vec{p}$ from the softmax mapping procedure discussed in section 2.2, w_i are the weights reflecting the relative importance of each objective, and F_i^{scale} are scaling factors, typically set to baseline values for normalization. The indices d, c and s are the dynamic, cost and structural identifiers, respectively. The scale and weight parameters used for the study case can be found in Table 1 and are picked based on preliminary analysis. Alternatively, this values can be assigned as the unscaled objective function values of a random run.

Table 1. Scale Parameters

F_c^{scale}	F_s^{scale}	F_d^{scale}	$w_s = w_d = w_c$
200,000	1	20	1

This reduces the multi-objective optimization to a mono-objective optimization problem, which can be solved using standard optimization algorithms.

2.2 Design parameters

In the optimization framework adopted in this study, the design parameters define the geometric and material configuration of the hybrid mooring line. These parameters are used to evaluate three performance aspects: the cost of the line, its dynamic response under environmental loading, and its structural safety. Each of these aspects is quantified by an individual objective function (f_c, f_d, f_s, respectively).

The overall optimization problem is originally multi-objective, since cost, dynamics, and safety can be conflicting design drivers. However, in this work the problem is reformulated into a single weighted objective function ((1)), obtained by normalizing and combining the three components. This allows the optimization to be solved with standard constrained algorithms while still reflecting the trade-offs among the objectives.

It is important to note that, in addition to contributing to the global objective, the structural safety function (f_s) is also enforced as a constraint. Specifically, the safety factor must remain above a predefined threshold (1.6 in this study), ensuring that only feasible configurations are considered. Similarly, the dynamic objective is

subject to a maximum displacement constraint (15 m), which prevents solutions that compromise station-keeping performance.

The design parameters $\vec{z}$ can be divided into two categories, the first being the relative lengths of each section of the mooring line $\vec{z^p}$, and the second being the unchanged input properties of each section $\vec{z^r}$. The design parameters are defined as follows:

The linear lengths $\vec{l}$ of each section s, where the total line length is given by $\sum_{s=1}^{N} l_s = L_o$, can be expressed as relative lengths using $\vec{p^p}_s = \frac{\vec{l}_s}{L_o}$. Since L_0 is a constant, the optimization problem can be reduced to optimizing the relative lengths of each section, where $\sum_{s=1}^{N^s} \vec{p^p}_s = 1$. To ensure this criterion is met, the optimization framework employs a softmax mapping function. The softmax mapping function can be expressed as

$$\vec{p^p}_s = \frac{e^{\vec{z^p}_s}}{\sum_{n=1}^{N^s} e^{\vec{z^p}_n}}, \tag{2}$$

where $\vec{z^p}$ are the input parameters for the parsed relative to section sizes parameters $\vec{p^p}$, and N^s is the number of sections in the mooring line. The softmax mapping function ensures that the relative lengths of each section are non-negative and sum to one, allowing for a well distributed design space across the standard simplex.

The second category of design parameters $\vec{z^r}$ includes the unaltered properties of each section. The model accepts the diameter d_s of each section s, and a slack value where $L_o = L \cdot slack$, with L being the geometric length. These parameters are not constrained by the softmax mapping function, allowing for independent optimization of each section's diameter and slack value. For the current study, the diameters are shared between the sections $d_s = d$, where d is the shared diameter, and the slack value is set to 1 and is unused as an optimization parameter for the taut-leg configuration.

Finally, the parsed input vector $\vec{p}$ is defined as a concatenation of the relative lengths $\vec{p^p}$ and the raw input $\vec{z^r} = d$ and is expressed as $\vec{p} \leftarrow \vec{z} = \left\{\vec{p^p}, \vec{z^r}\right\}$.

Cost objective function f_c

The cost objective f_c is expressed as the summation each section cost, which is calculated based on the linear cost c_s (USD/m) of each section material and their line lengths using

$$f_c(\vec{p}) = \sum (\vec{p^p}_s \cdot L_o) \cdot c_s, \tag{3}$$

where the linear costs are computed as discussed in section 3.

Dynamic objective function f_d

Two parameters are used to evaluate the dynamic behavior of the FOWT: the total displacement and the total rotation, which are computed from the OpenFAST dynamic simulation results as

$$f_d(\vec{p}) = |\vec{\Delta^t}| - \delta^{max} + |\vec{\Delta^r}|, \tag{4}$$

where δ^{max} is the project maximum displacement, set as 15 m for the study case, $\vec{\Delta^t}$ represents the total translational displacement of the FOWT, which is calculated as the square root of the sum of the squares of the sway, surge, and heave components as in

$$|\vec{\Delta^t}| = \sqrt{\text{sway}^2 + \text{surge}^2 + \text{heave}^2}. \tag{5}$$

Similarly, $\vec{\Delta^r}$ represents the total rotational displacement, which is calculated as the Euclidean distance of the pitch, roll, and yaw components in

$$|\vec{\Delta^r}| = \sqrt{\text{pitch}^2 + \text{roll}^2 + \text{yaw}^2}. \tag{6}$$

These parameters provide a measure of the dynamic response of the FOWT under varying environmental conditions, ensuring that the optimization framework accounts for both translational and rotational stability.

Structural objective function f_s

The structural objective function is defined as the maximum safety coefficient, which is computed as the fraction of the maximum tension in the simulation and the minimum breaking load (MBL) of a cable section. The minimum safety coefficient is set as a model constraint.

$$f_s(\vec{p}) = \max(\frac{\vec{F_i}}{M\vec{B}L_i}), \quad f_s(\vec{p}) < \frac{1}{S_f} \tag{7}$$

Here, $\vec{F_i}$ represents the maximum tension experienced by the i-th section of the mooring line during the simulation, while $M\vec{B}L_i$ is the minimum breaking load of the same section. The safety factor S_f is a predefined threshold that ensures the structural integrity of the mooring line by constraining the minimum allowable safety coefficient, a threshold of 1.6 is used in the study case. This constraint guarantees that the design remains within acceptable safety margins under operational and extreme conditions.

3 Material properties

The mooring line considered in this study is composed of two sections, each fabricated from distinct materials: high-modulus polyethylene (HMPE) and polyester. The mechanical and economic properties of these materials are parameterized as functions of the section diameter d, following the methodology implemented in the MoorPy library (Hall et al. [23]). This approach enables the evaluation of mass, strength, stiffness, and cost for each section based on its geometric characteristics. The constitutive model employed is linear elastic. Table 2 summarizes the Equations for key properties of each mooring line section as a function of diameter d, axial stiffness EA and minimum breaking load MBL.

Table 2. Section property equations as a function of diameter d (adapted from MoorPy Hall et al. [23]).

Property	**Equation**
Mass/length	$m = \alpha_m d^2$
MBL	$\sum \beta_i d^i$
Axial stiffness	$\sum \gamma_j d^j + \gamma_4 \,\mathrm{MBL}$
Cost/length	$\sum \delta_k d^k + \delta_4 m + \delta_5 EA + \delta_6 \,\mathrm{MBL}$

In these expressions, α_m, β_i, γ_j, and δ_k are material-specific coefficients determined empirically or from manufacturer data. The specific coefficients for polyester and HMPE, as adopted from MoorPy (Hall et al. [23]), are summarized in Table 3.

Table 3. Material property coefficients for polyester and HMPE mooring lines, as used in MoorPy version 1.1.0 (Hall et al. [23]).

Coefficient	**Polyester**	**HMPE**
α_m (mass_d2)	$679\ \mathrm{kg/m^3}$	$496\ \mathrm{kg/m^3}$
β_2 (MBL_d2)	$308 \times 10^6\ \mathrm{N/m^2}$	$580 \times 10^6\ \mathrm{N/m^3}$
β_3 (MBL_d3)	0	$651 \times 10^6\ \mathrm{N/m^2}$
γ_4 (EA_MBL)	14	56
δ_6 (cost_MBL)	$1.65 \times 10^{-5}\ USD/(\mathrm{m \cdot N})$	$1.4 \times 10^{-4}\ USD/(\mathrm{m \cdot N})$

The omitted coefficients are zero for both materials. Remaining material properties are set to the Moorpy default values for each material.

4 Test case: OC4 DeepCwind FOWT

The test case is based on the OC4 DeepCwind platform Robertson et al. [18] semi-submersible 5MW floating wind turbine shown in Figure 1. The structure is fixed to the seabed using a hybrid mooring line composed of two sections in series: a HMPE section and a polyester section. The optimization framework is applied to identify an optimal configuration of the mooring line to a prescribed maximum offset.

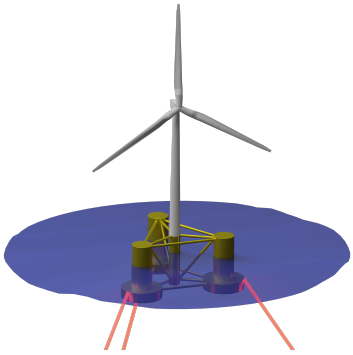


Figure 1. The OC4 DeepCwind 5MW FOWT. The turbine is facing the opposite direction (operational wind) from the simulations (extreme wind direction), where the back ($180°$) mooring leg is loaded while the others remain relaxed.

4.1 Mooring line configuration

The FOWT station-keeping system employs a hybrid mooring line composed of two sections, with the heavier cable (PET) placed at the bottom. To ensure stability, a maximum translational displacement of $15\,\mathrm{m}$ is imposed as a constraint during the optimization process. The main configuration is summarized in Table 4. Three mooring lines, each divided into two material sections, are arranged at heading angles of $60°$, $180°$, and $300°$ relative to the platform, providing symmetric station-keeping. The anchors are positioned at a radius of 840 m from the platform center. The fairlead points, where the mooring lines connect to the platform, are located at a depth of 14 m and a radial offset of 40.868 m from the center along the heading angles. Each mooring line is discretized into 80 elements for numerical simulation. To guarantee that each section contains at least one element, the number of elements per section is defined as $n_s = \left\lceil N_{\text{elements}} \cdot \vec{p}s \right\rceil$, where $N\text{elements} = 80$ is the total number of elements in the mooring line and $\vec{p}_s$ is the relative length of section s.

Table 4. Mooring line configuration parameters for the OC4 DeepCwind FOWT.

Parameter	**Value**
Water Depth	200 m
Line Heading Angles	$[60°, 180°, 300°]$
Anchor Radius	840 m
Fairlead Z Elevation	-14 m
Fairlead Radius	40.868 m
Number of Elements	80

4.2 Environmental conditions

The wave conditions are generated using the OpenFAST HydroDyn module with a white noise spectrum. The significant wave height is set to $1.788\,\mathrm{m}$ and the peak period is set to $10\,\mathrm{s}$. Table 5 summarizes the main sea state properties.

The wind conditions are generated using the OpenFAST AeroDyn module with a wind speed of $12\,\mathrm{m/s}$ at a reference height of $90\,\mathrm{m}$. Table 6 summarizes the main wind conditions used in the InflowWind simulation.

5 Results

To evaluate the performance of the proposed optimization framework, a series of simulations are conducted using OpenFAST. The optimization process was executed with the COBYLA algorithm, which is well-suited for constrained nonlinear optimization problems, as described by Abdelmoteleb and Bachynski-Polić [15], Leimeister

Table 5. Key sea state input conditions from HydroDyn SeaState file

Parameter	**Value**
Wave model (WaveMod)	White noise spectrum (3)
Significant wave height (WaveHs)	1.788 m
Peak spectral period (WaveTp)	10 s
Wave direction (WaveDir)	0°
Number of wave directions (WaveNDir)	1

Table 6. Main wind conditions used in InflowWind simulation

Parameter	**Value**
Wind type (WindType)	Steady (1)
Horizontal wind speed	12 m/s @ 90 m height
Wind propagation direction	0° (aligned with X-axis)
Upflow angle (VFlowAng)	0°
Power law exponent (PLExp)	0 (no shear profile)
Velocity interpolation in time	Linear

et al. [19]. The algorithm iteratively adjusts the design parameters to minimize the objective function while adhering to the specified constraints. A coarse mapping of the design parameters was employed to the selection of the initial conditions in Fig 2.

5.1 Solution mapping

Since COBYLA is not a global optimizer, the solution is sensible to the initial conditions. The solution mapping in 2 is used to determine candidate solutions for the problem. The evaluation is set at starting point of $\vec{p^p} = [50\%, 50\%]$ relative lengths and a line diameter of 80mm. Other tests using different starting points lead to different solutions lead to results in the valleys (dark blue) regions of the map in Figure 2. Despite that, those solutions provided similar results to the one provided in the next section.

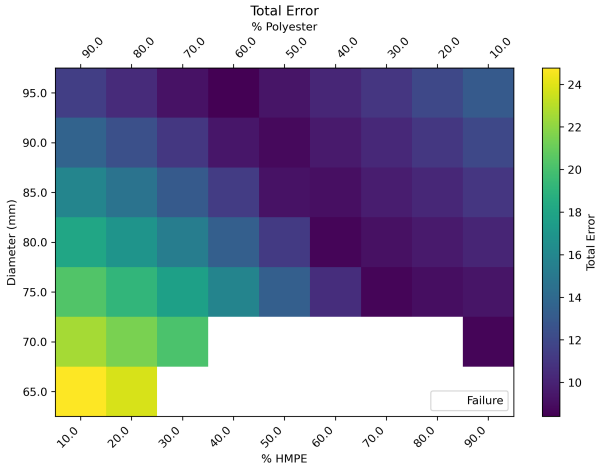


Figure 2. Total error by diameter and relative section sizes.

5.2 COBYLA results

The COBYLA optimization results are presented in Table 7. The Table reports the design parameters, objective function values, and computational times. The optimization process successfully converged to a solution that minimizes the total cost while maintaining acceptable performance metrics. Simulation times of 300 s are adopted for demonstration purposes. Real-world applications, however, should account for industry-standard environmental, safety, and simulation requirements.

Table 7. COBYLA optimization results

Setup	**Value**	**Result**	**Value**
Calls / Time	24 ($\sim$2 h)	f	8.6
Start	50% HMPE / 50% PET @ 80 mm	f_c	USD 868,668
Simulation	300 s	f_d	15 m
Final Design	60% HMPE / 40% PET @ 80 mm	f_s	1.91

Table 8. Line-section results obtained for the configuration analyzed from Table 7.

Parameter	**Relative Length**	**Length**	**Cost**	f_s
HMPE	60%	494 m	USD 836,946	3.91
Polyester	40%	326 m	USD 31,722	1.91

The identified sectional results for the solution can be seen in Table 8. Cost is computed according to Equation (3) using the cost model from Table 2 using the parameters from Table 3.

6 Conclusion

The optimization framework presented in this study provides a systematic approach for designing hybrid mooring lines for FOWTs. By combining multiple materials, the framework achieves a balance between cost, structural integrity, and dynamic performance. The use of OpenFAST for numerical simulations enables the evaluation of mooring line behavior under realistic environmental conditions. The results show that the proposed framework can identify locally optimal configurations for hybrid mooring lines, achieving significant cost reductions while preserving key performance metrics. Moreover, the findings suggest that hybrid material solutions are particularly promising under strict diameter and displacement constraints. Nonetheless, the current implementation is limited by the absence of global optimization strategies and a multi-objective formulation.

Future work may extend the framework by incorporating additional materials, refined failure criterion, more realistic mooring and environmental conditions, and longer simulation times. The integration of global multi-objective optimization algorithms and machine learning techniques may further enhance the design process; for instance, population-based algorithms can achieve global optimization and generate Pareto fronts rather than converging to a single optimum, as shown by Jiang [3], Leimeister et al. [19], Jiang et al. [21]. Overall, this study contributes to ongoing efforts to improve the sustainability and performance of offshore wind energy systems by demonstrating the viability of hybrid mooring lines for deepwater applications. The use of optimization algorithms such as COBYLA highlights their ability to rapidly converge to local minima, making them effective tools for fine-tuning design parameters, particularly in large-scale scenarios.

Acknowledgements. The authors would like to acknowledge the support of the GMAp group at UFRGS for providing the necessary resources and infrastructure for this research. Special thanks to the Moorpy and OpenFAST communities for their valuable contributions to the development of the simulation tools used in this study and to PROMEC and CAPES, for financing.

Authorship statement. The authors hereby confirm that they are the sole liable persons responsible for the authorship of this work, and that all material that has been herein included as part of the present paper is either the property (and authorship) of the authors, or has the permission of the owners to be included here.

References

[1] J. M. Jonkman. Dynamics of offshore floating wind turbines-model development and verification. *Wind Energy*, vol. 12, pp. 459–492, 2009.
[2] C. M. Wang, T. Utsunomiya, S. C. Wee, and Y. S. Choo. Research on floating wind turbines: A literature survey. *IES Journal Part A: Civil and Structural Engineering*, vol. 3, pp. 267–277, 2010.
[3] Z. Jiang. Mooring design for floating wind turbines: A review. *Renewable and Sustainable Energy Reviews*, vol. 212, pp. 115231, 2025.
[4] Y. Chevillotte. Characterization of the long-term mechanical behavior and the durability of polyamide mooring ropes for floating wind turbines, 2020.
[5] S. J. Banfield, N. F. Casey, and R. Nataraja. Durability of polyester deepwater mooring rope. *Proceedings of the Annual Offshore Technology Conference*, vol. 2005-May, pp. 1532–1542, 2005.
[6] M. B. Bastos. Improved high tenacity/high modulus polyester for stiffer mooring ropes. *OCEANS 2013 MTS/IEEE Bergen: The Challenges of the Northern Dimension*, vol. , 2013.
[7] M. B. Bastos, E. B. Fernandes, and A. L. N. D. Silva. Performance fibers for deep water offshore mooring ropes: Evaluation and analysis. *OCEANS 2016 - Shanghai*, 2016.
[8] da D. M. Cruz, de Ávila M. Barreto, L. Zangalli, C. E. M. Guilherme, F. T. Stumpf, and J. Vassoler. Hmpe fibers for offshore mooring systems: Experimental creep-rupture and lifetime prediction modeling. In *Proceedings of the XII Congresso Nacional de Engenharia Mecânica - CONEM 2024*. ABCM, 2024.
[9] F. T. Stumpf, de Ávila M. Barreto, da D. M. Cruz, and C. E. M. Guilherme. Numerical simulation of multi-material hybrid lines for offshore mooring. *Ocean Engineering*, vol. 305, pp. 117979, 2024.
[10] S. H. Sørum, N. Fonseca, M. Kent, and R. P. Faria. Modelling of synthetic fibre rope mooring for floating offshore wind turbines. *Journal of Marine Science and Engineering*, vol. 11, 2023.
[11] K. A. Ansari. Mooring with multicomponent cable systems. *Journal of Energy Resources Technology*, vol. 102, pp. 62–69. Catenária multi segmentos, 1980.
[12] S. Leite, L. Ropes, J. Boesten, and D. B. Dyneema. Otc 22486 hmpe mooring lines for deepwater modus, 2011.
[13] M. Hall, B. Buckham, and C. Crawford. Evaluating the importance of mooring line model fidelity in floating offshore wind turbine simulations. *Wind Energy*, vol. 17, pp. 1835–1853, 2014.
[14] M. Hall and A. Goupee. Validation of a lumped-mass mooring line model with deepcwind semisubmersible model test data. *Ocean Engineering*, vol. 104, pp. 590–603, 2015.
[15] S. E. Abdelmoteleb and E. E. Bachynski-Polić. A frequency-domain optimization procedure for catenary and semi-taut mooring systems of floating wind turbines. *Marine Structures*, vol. 101, pp. 103768, 2025.
[16] M. K. Al-Solihat and M. Nahon. Stiffness of slack and taut moorings. *Ships and Offshore Structures*, vol. 11, pp. 890–904, 2016.
[17] B. Jonkman, A. Platt, R. M. Mudafort, E. Branlard, L. Wang, D. Slaughter, M. Sprague, H. Ross, Hayman-Consulting, jjonkman, cortadocodes, M. Chetan, R. Davies, M. Hall, G. Vijayakumar, M. Buhl, reos rcrozier, Russell9798, P. Bortolotti, R. Bergua, S. Ananthan, J. Rood, rdamiani, nrmendoza, sinolonghai, A. Gupta, psakievich, F. H. Bhuiyan, pschuenemann, and A. Sharma. Openfast/openfast: v4.0.4, 2025.
[18] A. Robertson, J. Jonkman, M. Masciola, H. Song, A. Goupee, A. Coulling, and C. Luan. Definition of the semisubmersible floating system for phase ii of oc4. Technical report, National Renewable Energy Lab. (NREL), Golden, CO (United States), 2014.
[19] M. Leimeister, A. Kolios, and M. Collu. Development of a framework for wind turbine design and optimization. *Modelling 2021, Vol. 2, Pages 105-128*, vol. 2, pp. 105–128, 2021.
[20] I. A. Ja'e, M. O. A. Ali, A. Yenduri, Z. Nizamani, and A. Nakayama. Optimisation of mooring line parameters for offshore floating structures: A review paper. *Ocean Engineering*, vol. 247, pp. 110644, 2022.
[21] Y. Jiang, Y. Duan, J. Li, M. Chen, and X. Zhang. Optimization of mooring systems for a 10mw semisubmersible offshore wind turbines based on neural network. *Ocean Engineering*, vol. 296, pp. 117020, 2024.
[22] M. J. D. Powell. A Direct Search Optimization Method That Models the Objective and Constraint Functions by Linear Interpolation. In S. Gomez and J.-P. Hennart, eds, *Advances in Optimization and Numerical Analysis*, pp. 51–67, Dordrecht. Springer Netherlands, 1994.
[23] M. Hall, S. Housner, S. Sirnivas, and S. Wilson. Moorpy (quasi-static mooring analysis in python). [Computer Software] `https://doi.org/10.11578/dc.20210726.1`, 2021.